Inorg. Chem. **2004**, *43*, 2636–2642

Synthesis, Structure, and Magnetic Properties of Amine-Templated Open-Framework Nickel(II) Sulfates

J. N. Behera,[†] K. V. Gopalkrishnan,[‡] and C. N. R. Rao*[,†]

Chemistry and Physics of Materials Unit, Jawaharlal Nehru Centre for Advanced Scientific Research, Jakkur P. O., Bangalore 560064, India, Solid State and Structural Chemistry Unit, Indian Institute of Science, Bangalore 560012, India, and Department of Condensed Matter Physics and Materials Science, Tata Institute of Fundamental Research, Mumbai, 400005, India

Received December 26, 2003

Two organically templated nickel sulfates of the compositions $[C_4N_2H_{12}][Ni_3F_2(SO_4)_3(H_2O)_2]$ (**I**) and $[C_4N_2H_{12}][Ni_2F_4(SO_4)H_2O]$ (**II**) with open architectures have been synthesized under hydro/solvothermal conditions in the presence of piperazine. **I** has a layered structure formed by sinusoidal chains comprising hexameric units, whereas **II** has a three-dimensional structure with 10-membered channels. The layered Ni(II) sulfate, **I**, is ferrimagnetic, exhibiting hysteresis at low temperatures. The three-dimensional Ni(II) sulfate, **II**, is essentially paramagnetic. We have also obtained layered compounds isostructural with **I** containing other amines.

Introduction

Inorganic open-framework structures involving silicates,[1] phosphates,[2] and carboxylates[3,4] have been widely investigated in the past few years. It has been demonstrated recently that oxyanions such as selenite,[5] selenate,[6] and sulfate[7] can also be made use of to build up open architectures. Accordingly, several layered sulfates of iron and cobalt have been reported,[7] but no three-dimensional transition metal sulfate appears to be known. Among the transition metal sulfates, layered or 3-dimensional nickel sulfates have not been synthesized hitherto. Three-dimensional organically templated sulfates of uranium,[8] lanthanum,[9] and scandium,[10] however, have been reported recently. We have been able to prepare both layered and 3-dimensional nickel sulfates employing piperazine as the structure-directing agent. In this article, we report the synthesis, structure, and magnetic properties of $[C_4N_2H_{12}][Ni_3F_2(SO_4)_3(H_2O)_2]$, **I**, and $[C_4N_2H_{12}][Ni_2F_4(SO_4)H_2O]$, **II**, containing piperazine. Interestingly, **I** with the layered structure exhibits ferrimagnetism, whereas the three-dimensional **II** is essentially paramagnetic. We have also been able to prepare compounds isomorphous with **I** using other amines. The observation of well-defined ferrimagnetic properties with magnetic hysteresis in **I** as well as the three-dimensional structure of **II** is noteworthy.

Experimental Section

Synthesis and Characterization. Compounds **I** and **II** were synthesized by employing mild hydro/solvothermal methods in the presence of organic amines. Compound **I** was synthesized as

* To whom correspondence should be addressed. E-mail: cnrrao@jncasr.ac.in. Fax: +91-80-8462766.

[†] Jawaharlal Nehru Centre for Advanced Scientific Research and Indian Institute of Science.

[‡] Tata Institute of Fundamental Research.

(1) (a) Breck, D. W. *Zeolite Molecular Sieves*; Wiley: New York, 1974. (b) Meier, W. M.; Oslen, D. H.; Baerlocher, C. *Atlas of Zeolite Structure Types*; Elsevier: London, 1996.

(2) Cheetham, A. K.; Ferey, G.; Loiseau, T. *Angew. Chem., Int. Ed.* **1999**, *38*, 3268. (b) Rao, C. N. R.; Natarajan, S.; Choudhury, A,; Neeraj, S.; Ayi, A. A. *Acc. Chem. Res*. **2001**, *34*, 80.

(3) (a) Livage, C.; Egger, C.; Ferey, G. *Chem. Mater.* **1999**, *11*, 1546. (b) Reinke, T. M.; Eddaoudi, M.; O'Keeffe, M.; Yaghi, O. M. *Angew. Chem., Int. Ed.* **1999**, *38*, 2590 and references therein. (c) Li, H.; Eddaoudi, M.; Groy, T. L.; Yaghi, O. M. *J. Am. Chem. Soc*. **1998**, *120*, 8571.

(4) (a) Guillou, N.; Pastre, S.; Livage, C.; Ferey, G. *Chem. Commun*. **2002**, 2358. (b) Vaidhyanathan, R.; Natarajan, S.; Rao, C. N. R. *Chem. Mater*. **2001**, *13*, 185.

(5) (a) Choudhury, A.; Udayakumar, D.; Rao, C. N. R. *Angew. Chem., Int. Ed.* **2002**, *41*, 158 (b) Harrison, W. T. A.; Philips, M. L. F.; Stanchfield, J.; Nenoff, T. M. *Angew. Chem., Int. Ed.* **2002**, *39*, 3808. (c) Udayakumar, D.; Rao, C. N. R. *J. Mater. Chem*. **2003**, *13*, 1635.

(6) (a) Pasha, I.; Choudhury, A.; Rao, C. N. R. *J. Solid State Chem*. **2003**, *174*, 386. (b) Udayakumar, D.; Dan, M,; Rao, C. N. R. *Eur. J. Inorg. Chem.* **2004** (in press).

(7) (a) Paul, G.; Choudhury, A.; Sampathkumaran, E. V.; Rao, C. N. R. *Angew. Chem., Int End.* **2002**, *41*, 4297. (b) Behera, J. N.; Paul, G.; Choudhury, A.; Rao, C. N. R. *Chem. Commun.* **2004**, 456. (c) Paul, G.; Choudhury, A.; Rao, C. N. R. *Chem. Mater*. **2003**, *15*, 1174. (d) Paul, G.; Choudhury, A.; Nagarajan, R.; Rao, C. N. R. *Inorg. Chem*. **2003**, *42*, 2004. (e) Paul, G.; Choudhury, A.; Rao, C. N. R. *J. Chem. Soc., Dalton Trans.* **2002**, 3859.

(8) Doran, M. Norquist, A. J.; O'Hare, D. *Chem. Commun*. **2002**, 2946.

(9) Bataille, T.; Louer, D. *J. Mater. Chem*. **2002**, *12*, 3487.

(10) Bull, I.; Wheatley, P. S.; Lightfoot, P.; Morris, R. E.; Sastre, E.; Wright, P. A. *Chem. Commun.* **2002**, 1180.

10.1021/ic035488u CCC: $27.50
Published on Web 03/18/2004

follows. NiO (0.074 g) was dissolved in an ethylene glycol (EG)/H_2O mixture (4.6 and 0.9 mL, respectively) under constant stirring. To this solution was added 0.16 mL of H_2SO_4 (98%) and 0.2 mL of HF (48%). Finally, 0.258 g of piperazine (PIP) was added to the mixture, and the mixture was stirred for 1 h to obtain a homogeneous gel. The final mixture with the molar composition of $NiO/H_2SO_4/HF/PIP/EG/H_2O$ (1:3:2:3:50:50) was transferred into a 23-mL Teflon-lined acid digestion bomb and heated at 180 °C for 3 days under autogenous pressure. The product containing green needle-shaped crystals was monophasic (yield 80% with respect to Ni).

Compound **II** was prepared by employing piperazine sulfate as the source of the sulfate and the amine. Piperazinium sulfate $[H_3N(CH_2)_4NH_3]SO_4 \cdot H_2O$ (PIPS) was prepared following the procedure reported in the literature.[11] In a typical synthesis, 0.148 g of NiO was dispersed in an ethanol/water mixture under constant stirring. To this mixture, 0.502 g of PIPS and 0.2 mL of HF were added and the mixture was stirred for 1 h. The final mixture with the molar composition of NiO/PIPS/HF/H_2O/ethanol (2:2.5:3:50:50) was transferred into a 7-mL Teflon-lined acid digestion bomb and heated at 180 °C for 48 h to obtain green needle-shaped crystals (yield 65%).

Initial characterization of **I** and **II** was carried out by powder X-ray diffraction (PXRD), energy dispersive analysis of X-rays (EDAX), chemical analysis, thermogravimetric analysis (TGA), and IR spectroscopy. Magnetic measurements on powdered samples were performed at temperatures between 2 and 300 K, using a Quantum Design SQUID magnetometer. The PXRD pattern exclusively exhibited reflections of a hitherto unknown material; and was consistent with the structure determined by single-crystal XRD, which gave the compositions of **I** and **II** as $[C_4N_2H_{12}][Ni_3F_2(SO_4)_3(H_2O)_2]$ and $[C_4N_2H_{12}]\ Ni_2F_4(SO_4)\ H_2O]$, respectively. Both the nickel sulfates gave satisfactory elemental analysis. The experimental and calculated (in wt %) values of C, H, N were as follows. **I**: C, 7.4; N, 4.1; H, 3.7 (calc.: C, 7.6; N, 4.4; H, 2.3). **II**: C, 11.5; N, 6.8; H, 5 (calc.: C, 12.1; N, 7; H, 3.6). EDAX indicated the ratios of Ni and S to be 1:1 in **I** and 2:1 in **II**, in agreement with the molecular formulas. Quantitative analysis of nickel for **I** was 27.3% (calc. 29.6%) and 27.2% for **II** (calc. 28.1%). The sulfate content was found to be 44.6% in **I** and 23.8% in **II** compared to 45.8% and 24.2% expected on the basis of the formulas. TGA showed loss of water corresponding to two and one water molecules, respectively, in **I** and **II** (TGA data are provided as Supporting Information). These analytical data confirm the molecular formulas of **I** and **II** from crystallography and their fluorine content as shown.

In the TGA curve of **I**, there was a two-step weight loss corresponding to the loss of the water in the range 130 to 170 °C [obs, 5.26%; calc, 5.21%] and to the loss of amine, HF, and SO_3 in the range 300 to 550 °C [obs, 57.7%; calc, 56.4%]. The PXRD pattern of the sample heated to 900 °C corresponded to Ni_3S_2 (JCPDS file card 44-1418). In **II**, there was a four-step weight loss: of water at 125−180 °C [obs, 5.5%; calc, 4.6%], of the amine at 300 °C [obs, 22.6%; calc, 22.3%], of HF and F_2 at 380 °C [obs, 21.1%; calc, 19.7%], and of SO_2 at 450 °C [obs, 17.2%; calc, 16.4%]. The PXRD pattern of the sample heated to 900 °C corresponded to NiO (JCPDS file card 22-1189). Infrared spectra of **I** and **II** showed characteristic bands in the 980−1010 cm^{-1} region due to ν_1 and in the 1090−1140 cm^{-1} region due to ν_3 of the sulfate group.[12] The bending mode of SO_4^{2-} was in the 450−600 cm^{-1} region. The stretching and bending modes of N−H and O−H bands were in the expected range.

Table 1. Crystal Data and Structure Refinement Parameters for Compounds **I** and **II**

empirical formula	$C_4H_{16}Ni_3F_2N_2O_{14}S_3$ (**I**)	$C_4\ H_{12}F_4N_2Ni_2O_5S$ (**II**)
formula mass	626.47	395.65
crystal system	orthorhombic	tetragonal
space group	*Pnma* (62)	*P4*(1) (76)
a (Å)	9.9255(8)	10.8722(2)
b (Å)	22.137(2)	10.8722(2)
c (Å)	7.2316(6)	8.9098(2)
volume (Å^3)	1588.9(2)	1053.18(4)
Z	4	4
T (°C)	20	20
λ (Mo Kα) (Å)	0.71073	0.71073
ρ_{calc} (gcm^{-3})	2.619	2.495
μ (mm^{-1})	4.018	3.849
R [$I > 2\sigma(I)$]	R1 = 0.0342, wR2 = 0.0778	R1= 0.0301,wR2 = 0.0649
R (all data)	R1[a]= 0.0472, wR2[b]= 0.0841	R1[a]= 0.0350, wR2[b]= 0.0668

[a] $R_1 = \sum|F_0| - |F_c|$; [b] $wR_2 = \{[w(F_0^2 - F_c^2)^2]/[w(F_0^2)^2]\}^{1/2}$, $w = 1/[\sigma^2(F_0)^2 + (aP)^2 + bP]$, $P = [F_0^2 + 2Fc^2]/3$; where $a = 0.0454$ and $b = 0$ for **I**, and $a = 0.0207$ and $b = 0$ for **II**.

Single-Crystal Structure Determination. A suitable single crystal of each compound was carefully selected under a polarizing microscope and mounted at the tip of the thin glass fiber using cyanoacrylate adhesive (super glue). Single-crystal structure determination by X-ray diffraction was performed on a Siemens SMART-CCD diffractometer equipped with a normal focus, 2.4-kW, sealed-tube X-ray source (Mo Kα radiation, $\lambda = 0.71073$Å) operating at 40 kv and 40 mA. The structure was solved by direct methods using SHELXS-86,[13] which readily revealed all the heavy atom positions (Ni, S) and enabled us to locate the other non-hydrogen (C, N, O, and F) positions from the difference Fourier maps. An empirical absorption correction based on symmetry equivalent reflections was applied using SADABS.[14] All the hydrogen positions were found in the difference Fourier maps. For the final refinement, the hydrogen atom of both the framework and the amine were placed geometrically and held in the riding mode. The last cycles of refinement included atomic positions; anisotropic thermal parameters for all the non-hydrogen atoms and isotropic thermal parameters for all the hydrogen atoms. Full-matrix least-squares structure refinement against $|F^2|$ was carried out using the SHELXTL-PLUS[15] package of programs. Details of the structure determination and final refinements for **I** and **II** are listed in Table 1. The positions of the fluorine atoms of **I** and **II** are located primarily looking at their thermal parameters; assigning them as oxygens instead of fluorine invariably leads to nonpositive definite values when they were refined with anisotropic displacement parameters. X-ray diffraction patterns of **I** and **II** were in good agreement with the simulated patterns based on single-crystal data, indicative of their phase purity.

Results and Discussion

Layered $[C_4N_2H_{12}][Ni_3F_2(SO_4)_3(H_2O)_2]$, I. The asymmetric unit of **I** contains 17 non-hydrogen atoms, of which 14 belong to the inorganic framework and 3 belong to the

(11) Jayaraman, K.; Choudhury, A.; Rao, C. N. R. *Solid State Sci.* **2002**, *4*, 413.
(12) Nakamato, K. *Infrared and Raman Spectra of Inorganic and Coordination Compounds*; Wiley-Interscience: New York, 1978.
(13) Sheldrick, G. M. *SHELXS-86 Program for Crystal Structure Determination*; University of Gottingen: Gottingen, Germany, 1986. (b) Sheldrick, G. M. *Acta Crystallogr., Sect. A* **1990**, *46*, 467.
(14) Sheldrick, G. M. *SADABS*: *Siemens Area Detector Absorption Correction program*; University of Gottingen: Gottingen, Germany, 1994.
(15) Sheldrick, G. M. *SHELXTL-PLUS Program for Crystal Structure Solution and Refinement*; University of Gottingen: Gottingen, Germany.

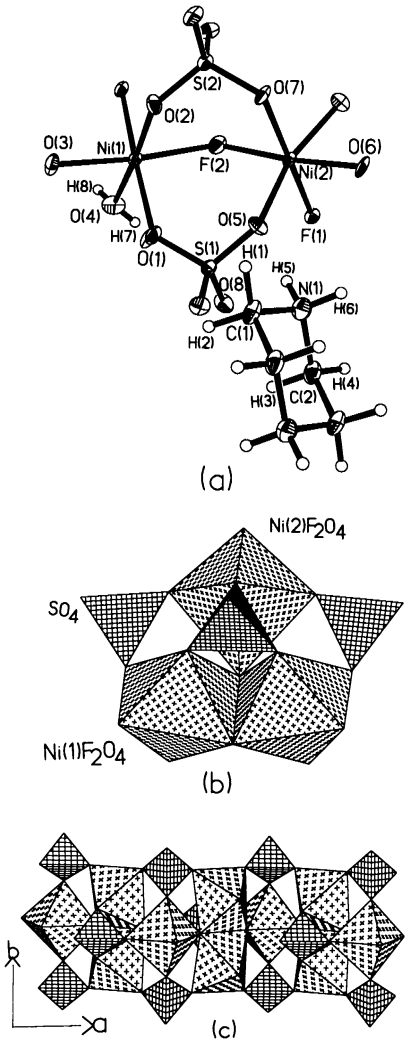

Figure 1. (a) ORTEP plot of $[C_4N_2H_{12}][Ni_3F_2(SO_4)_3(H_2O)_2]$, **I**. The asymmetric unit is labeled. Thermal ellipsoids are given at 50% probability. (b) Polyhedral representation of the hexameric units in **I**. Note the presence of two four-membered and one three-membered rings. (c) The infinite chain formed by the connectivity of the hexameric units.

extraframework amine molecule (Figure 1a). There are two crystallographically distinct Ni and S atoms, of which one nickel and one sulfur atom [Ni(1) and S(1)] are in special positions with an occupancy of 0.5. The structure of **I** is constructed from macroanionic inorganic framework layers of $[Ni_3F_2(SO_4)_3(H_2O)_2]^{2-}$ held together by strong hydrogen bonds with the amine molecules residing in the interlamellar space. The Ni atoms in **I** are octahedrally coordinated to four oxygens and two fluorine atoms. The Ni−O/F bond distances are in the range 2.065(5)−2.129(5) Å and O/F−Ni−O/F bond angles in the range 79.72(12)−179.5(2)°. Of the two sulfur atoms, S(2) has four S−O−Ni linkages and S(1) has three such connections, with one terminal S(1)−O(4) bond. The S−O bond distances are in the range 1.471(4)−1.487(4) Å and the average O−S−O bond angle is 108.2°. Bond valence sum calculations for **I** based on the method of Brown and Altermatt,[16] using r_0 (Ni−F) =1.596 and r_0 (Ni−O) = 1.670 Å, show that the valence sums for Ni(1) = 1.98, Ni(2) = 1.92 Å and F(1) = 0.606, F(2) = 0.563. The charges on Ni and S are clearly +2 and +6, respectively. These data are consistent with the stated composition and the presence of fluorine. Selected bond distances and angles of **I** are listed in Table 2.

(16) Brown, I. D.; Altermatt, D. *Acta Crystallogr*. **1985**, *B47*, 244.

Table 2. Selected Bond Distances and Angles in **I**[a]

Bond Distances

moiety	distance (Å)	moiety	distance (Å)
Ni(1)−O(1)	2.026(4)	Ni(2)−F(2)	2.048(4)
Ni(1)−O(2)	2.048(4)	O(1)−S(1)	1.480(4)
Ni(1)−O(3)	2.058(4)	O(3)−S(1)#1	1.487(4)
Ni(1)−O(4)	2.055(5)	O(5)−S(1)	1.471(4)
Ni(1)−F(1)#1	2.061(3)	O(8)−S(1)	1.447(4)
Ni(1)−F(2)	2.082(3)	O(2)−S(2)	1.474(4)
Ni(2)−O(5)	2.011(4)	O(6)−S(2)#5	1.461(5)
Ni(2)−O(5) #2	2.011(4)	O(7)−S(2)	1.475(5)
Ni(2)−O(6)	2.060(5)	O(4)−H(7)	0.70(11)
Ni(2)−O(7)	2.129(5)	O(4)−H(8)	0.77(6)
Ni(2)−F(1)	2.015(4)		

Bond Angles

moiety	angle(deg)	moiety	angle(deg)
O(1)−Ni(1)−O(2)	95.9(2)	F(2)−Ni(2)−O(7)	91.3(2)
O(1)−Ni(1)−O(4)	87.8(2)	O(6)−Ni(2)−O(7)	81.0(2)
O(1)−Ni(1)−O(3)	85.3(2)	S(1)−O(1)−Ni(1)	135.0(2)
O(2)−Ni(1)−O(3)	84.0(2)	S(2)−O(2)−Ni(1)	126.5(2)
O(2)−Ni(1)−O(4)	175.8(2)	S(1)#1−O(3)−Ni(1)	132.4(2)
O(4)−Ni(1)−O(3)	94.2(2)	Ni(2)−F(1)−Ni(1)#3	129.10(9)
O(1)−Ni(1)−F(1)#1	174.2(2)	Ni(1)#3−F(1)−Ni(1)#4	99.6(2)
O(2)−Ni(1)−F(1)#1	88.6(2)	Ni(2)−F(2)−Ni(1)	119.42(14)
O(3)−Ni(1)−F(1)#1	98.79(14)	Ni(1)−F(2)−Ni(1)#2	98.3(2)
O(4)−Ni(1)−F(1)#1	87.9(2)	S(1)−O(5)−Ni(2)	132.9(2)
O(1)−Ni(1)−F(2)	96.74(14)	S(2)#5−O(6)−Ni(2)	146.5(3)
O(2)−Ni(1)−F(2)	88.0(2)	S(2)−O(7)−Ni(2)	120.4(3)
O(3)−Ni(1)−F(2)	172.0(2)	O(8)−S(1)−O(5)	108.8(2)
O(4)−Ni(1)−F(2)	93.6(2)	O(8)−S(1)−O(1)	109.8(2)
F(1)#1−Ni(1)−F(2)	79.72(12)	O(5)−S(1)−O(1)	110.7(2)
F(1)−Ni(2)−F(2)	88.2(2)	O(8)−S(1)−O(3)#4	110.5(2)
O(5)−Ni(2)−F(1)	89.70(11)	O(5)−S(1)−O(3)#4	109.4(2)
O(5)−Ni(2)−F(2)	98.23(11)	O(1)−S(1)−O(3)#4	107.6(2)
O(5)−Ni(2)−O(6)	81.92(11)	O(6)#6−S(2)−O(2)	107.5(2)
F(1)−Ni(2)−O(6)	99.6(2)	O(2)−S(2)−O(2)#2	111.2(3)
F(2)−Ni(2)−O(6)	172.2(2)	O(6)#6−S(2)−O(7)	110.8(3)
O(5)−Ni(2)−O(7)	90.38(11)	O(2)−S(2)−O(7)	109.9(2)
F(1)−Ni(2)−O(7)	179.5(2)		

[a] Symmetry transformations used to generate equivalent atoms: #1 $^1/_2$, y, $-z + ^1/_2$; #2 x, $-y + ^1/_2$, z; #3 $x - ^1/_2$, $-y + ^1/_2$, $-z + ^1/_2$; #4 $x - ^1/_2$, y, $-z + ^1/_2$; #5 $x - ^1/_2$, y, $-z + ^3/_2$; #6 $x + ^1/_2$, y, $-z + ^3/_2$; #7 $-x + 1$, $-y + 1$, $-z + 2$.

The framework of **I** is built up of $Ni(1)F_2O_4$, $Ni(2)F_2O_4$ octahedra and SO_4 tetrahedra sharing edges as Ni−μ−F−Ni bonds and vertexes as Ni−O−S bonds. The $Ni(1)F_2O_4$ octahedra are dimerized by sharing edges with two fluorines (F_1 and F_2) to form $Ni_2F_2O_8$ moiety. $Ni(2)F_2O_4$ octahedra link to the anion at one end of the shared edges to form trimeric $Ni_3F_3O_{12}$ units. The $S(1)O_4$ tetrahedra cap the trimers from both ends while the $S(2)O_4$ tetrahedra are grafted on to the trimers in such a way that they share three corners with three octahedra, giving rise to the hexameric unit as shown in Figure 1b. The connectivity of the octahedra and tetrahedra inside the unit results in two four-membered and one three-membered ring. These units are connected to one another through corner-sharing Ni−O−S linkages, thereby forming the sinusoidal chain shown in Figure 1c. Such chains run along the [010] direction and are covalently bonded to each other by the $S(2)O_4$ group forming the layer structure.

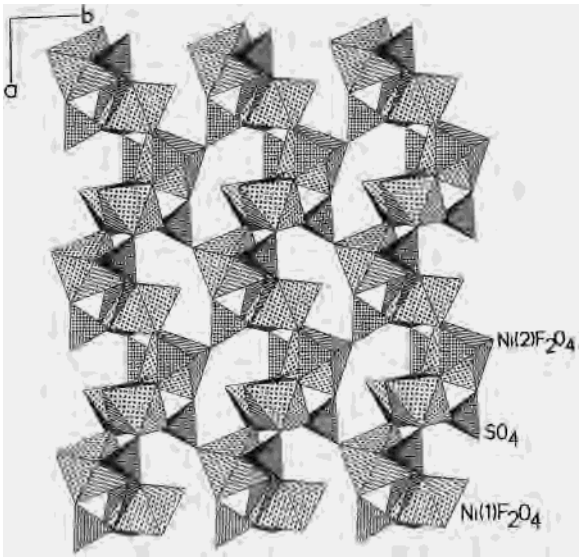

Figure 2. Polyhedral representation of the inorganic layer in **I** in the *ab*-plane. Note the presence of eight-membered apertures.

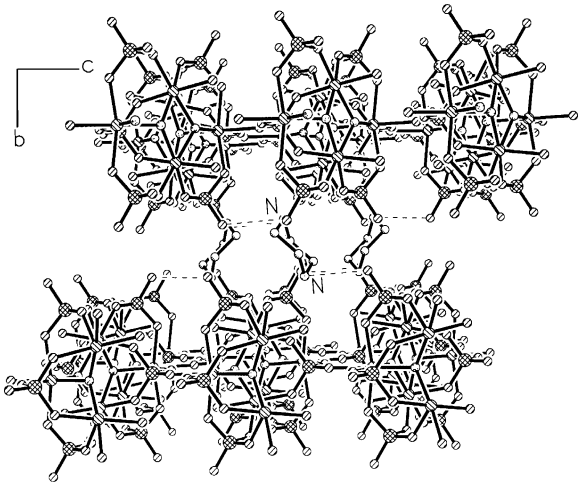

Figure 3. View down the crystallographic *a*-axis showing the packing of layers in **I**. Hydrogen bonding interactions between the amine and the framework oxygen are shown by dotted lines.

The $S(2)O_4$ tetrahedra from the adjacent chains connect alternatively via four Ni−O−S linkages to form four connected tetrahedra, leading to the formation of an eight-membered aperture in the *ab*-plane (shown in Figure 2). The inorganic layers are stacked along the *c*-axis in the ABAB fashion and the interlayer space is occupied by the diprotonated amine, which ensures the stability of the structure through extensive hydrogen bonding as shown in Figure 3. The structure can be compared to the mineral sulfoborite[17] which is made up of complex sheets of (MgO_6) and (SO_4) tetrahedra. In the mineral amarantite, octahedral tetramers are polymerized to form octahedral chains parallel to [100] and linked by (SO_4) tetrahedra, with the linkage between sheets being provided by [$B(OH)_4$] tetrahedra.

We have obtained nickel sulfates with a structure similar to that of **I** by using DABCO and 1,3-diaminopropane (DAP) as well, the only difference being that the compound with 1,3-diaminopropane has three crystallographically distinct Ni and S atoms in the asymmetric unit instead of two and has contained one additional lattice water. The presence of different amines in the interlamellar space causes the materials to be crystallized in different space groups. The crystallographic details are listed in Table 3. The structures of the DABCO- and DAP-derived Ni(II) sulfates are given in Figure 4.

Table 3. Crystal Structures of Other Amine-Templated Nickel Sulfates Structurally Analogous to **I**

parameter	1,3-DAP[c]	DABCO[d]
empirical formula	$C_3H_{18}Ni_3F_2N_2O_{15}S_3$	$C_6H_{18}Ni_3F_2N_2O_{14}S_3$
formula mass	632.50	652.49
crystal system	monoclinic	orthorhombic
space group	*Pc* (7)	*Pbcm* (57)
a (Å)	9.8933	7.4812
b (Å)	7.3387	9.8553
c (Å)	11.9891	24.0836
β (Å)	97.977	
volume (Å)	862.03	1775.67
Z	2	8
T (°C)	20	20
λ(Mo Kα) (Å)	0.71073	0.71073
ρ_{calc} (gcm^{-3})	2.421	2.435
μ (mm^{-1})	3.683	3.592
R [$I > 2\sigma(I)$]	R1 = 0.0467, wR2 = 0.0999	R1 = 0.0449, wR2 = 0.1001
R (all data)	R1[a] = 0.0676, wR2[b] = 0.1280	R1[a] = 0.0729, wR2[b] = 0.1144

[a] $R_1 = \sum|F_0| - |F_c|$; [b] $wR_2 = \{[w(F_0^2 - F_c^2)^2]/[w(F_0^2)^2]\}^{1/2}$, $w = 1/[\sigma^2(F_0)^2 + (aP)^2 + bP]$, $P = [F_0^2 + 2Fc^2]/3$; where $a = 0.0565$ and $b = 2.0499$ for DAP, and $a = 0.0604207$ and $b = 0$ for DABCO. 1,3-DAP[c] = 1,3-diaminopropane; DABCO[d] = 1,4-Diazabicyclo[2.2.2]octane.

We show the variable temperature magnetic susceptibility (χ) data of **I** recorded at 5000 Oe in Figure 5. In the paramagnetic region, the susceptibility follows the Curie−Weiss law with a negative Curie temperature of −74K as obtained from the fit of the χ_M^{-1} data in the 100−300 K range (inset of Figure 5). The negative θ value suggests that the exchange interaction is antiferromagnetic. The effective magnetic moment of Ni is 3.14 μ_B, comparable to that of nickel(II) compounds reported in the literature.[18,19] The data in Figure 5 also show a magnetic transition at low temperature. The dc magnetic susceptibility data under zero-field-cooled (ZFC) and field-cooled (FC) conditions (100 Oe) clearly show divergence (Figure 6), suggesting that the low temperature transition is ferrimagnetic. Interestingly **I** shows good magnetic hysteresis at 5 K (see inset of Figure 6). Complete saturation occurs at fairly high fields.

Three-Dimensional [$C_4N_2H_{12}$][$Ni_2F_4(SO_4)\ H_2O$], II. The nickel sulfate **II** is a three-dimensional network structure made up of $Ni(1)F_4O_2$, $Ni(2)F_4O_2$ octahedra, and SO_4 tetrahedra incorporating diprotonated piperazine molecules within the pores. The asymmetric unit of **II** consists of 17 non-hydrogen atoms, of which 11 belong to the inorganic framework and 6 belong to the guest as shown in the Figure 7a. There are two crystallographically distinct Ni atoms and one S atom with both the nickel atoms in octahedral coordination with respect to the O/F neighbors. The Ni−O

(17) Hawthrone, F. C.; Krivovichev, S. V.; Burns, P. C. *Rev. Miner. Geochem.* **2000**, *40*, 55.

(18) Gao, Q.; Guillou, N.; Nogues, M.; Cheetam, A. K.; Ferey, G. *Chem. Mater.* **1999**, *11*, 2937.

(19) Guillou, N.; Gao, Q.; Nogues, M.; Cheetam, A. K.; Ferey, G. *Solid State Sci.* **2002**, *4*, 1179.

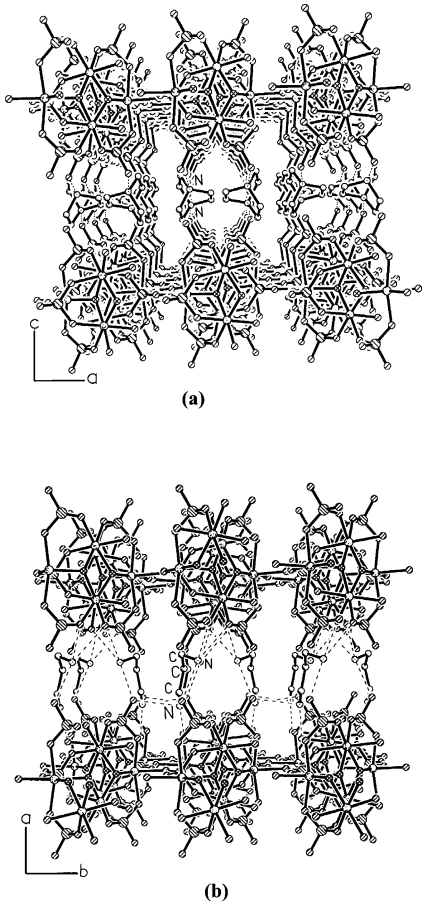

Figure 4. Structures of Ni(II) sulfates isomorphous with **I** obtained with (a) DABCO and (b) 1,3-diaminopropane (DAP).

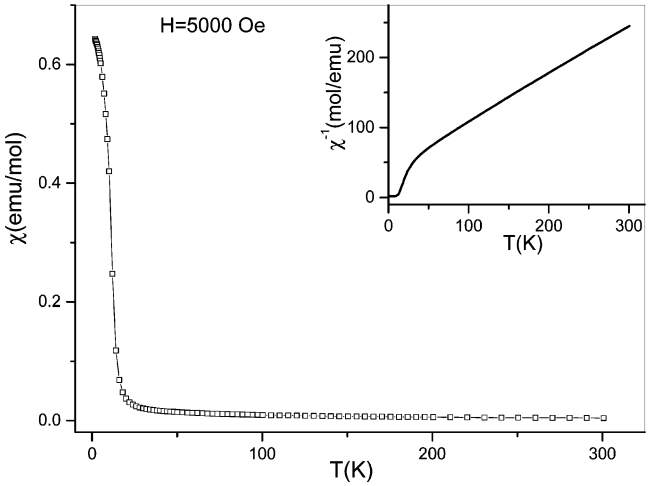

Figure 5. Temperature variation of the magnetic susceptibility of **I**. Inset shows the variation of inverse susceptibility.

bond distances are in the range 2.097(4)−2.030(4) Å [Ni(1)−O_{av} = 2.059, Ni(2)−O_{av} = 2.066 Å]. Ni−F bond distances are in the range 1.987(4)−2.059(4) Å [Ni(1)−F_{av} = 2.033, Ni(2)−F_{av} = 2.016 Å]. The trans F/O−Ni−O/F bond angles are in the range 175.9(2)−168.7(2)° and the cis F/O−Ni −O/F angles are in the range 78.89(14)−101.1(2)° with averages of 172.4 and 85.06°, respectively. Selected bond distances and angles in **II** are listed in Table 4. Of the two Ni atoms, Ni(1) makes four Ni−F−Ni bonds and one

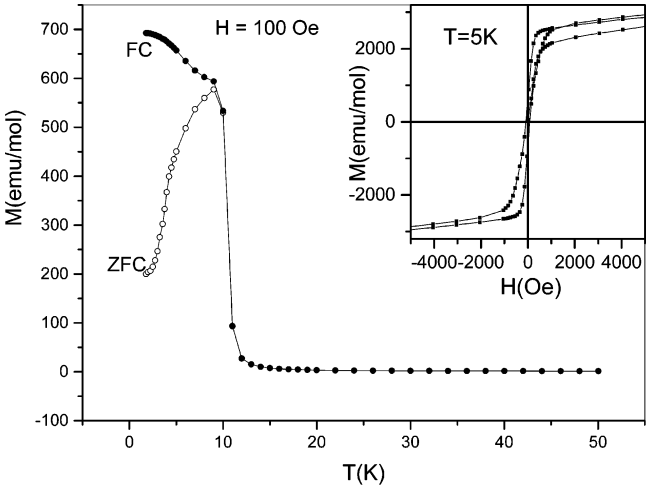

Figure 6. Temperature dependence of the DC magnetic susceptibility of **I** measured at 100 Oe under field-cooled (FC) and zero-field-cooled (ZFC) conditions. The hysteresis loop is shown in the inset.

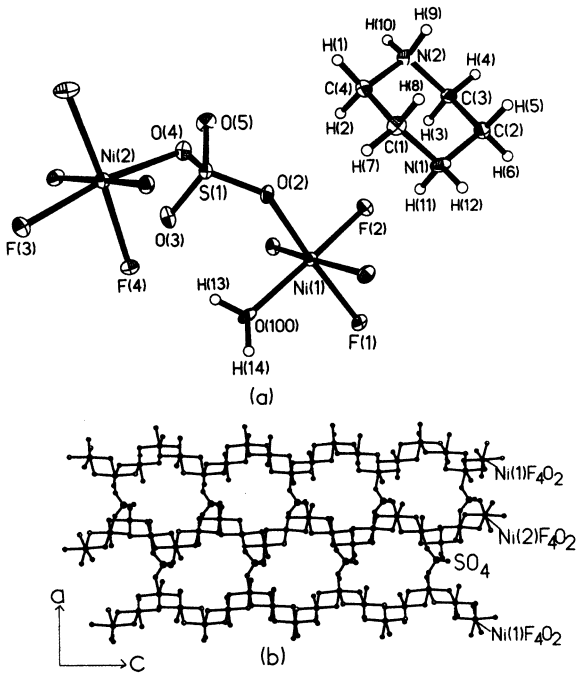

Figure 7. (a) ORTEP plot of $[C_4N_2H_{12}][Ni_2F_4SO_4(H_2O)_2]$, **II**. The asymmetric unit is labeled. Thermal ellipsoids are given at 50% probability. (b) Layer in the *ac*-plane formed by the infinite chains. Note the presence of 11-membered rings.

Ni−O−S linkage, with the sixth coordination being completed by linking to a H_2O molecule. Ni(2) forms four Ni−F−Ni and two Ni−O−S linkages. The fluorine atoms act as a bridge between the Ni centers, similar to that in phosphates of nickel and iron reported in the literature.[20,21] The unique S atom is tetrahedrally coordinated by the oxygen neighbors with the S−O bond distance ranging between 1.489(4) and 1.459(4) with an average bond distance of 1.474 Å. The S-atom makes three S−O−Ni linkages and the fourth one is terminal. Bond-valence sum (BVS) calculations (Ni-

(20) Liu, Y.; Zhang, L.; Shi, Z.; Yuan, H.; Pang, W. *J. Solid State Chem.* **2001**, *158*, 68.
(21) Mandal, S.; Natarajan, S.; Greneche, J. M.; Riou-Cavellec, M.; Ferey, G. *Chem. Mater.* **2002**, *14*, 3751.

Table 4. Selected Bond Distances and Angles for $[C_4N_2H_{12}][Ni_2F_4SO_4(H_2O)]$ **II**[a]

Bond Distances			
moiety	distance (Å)	moiety	distance (Å)
Ni(1)−F(1)	20.030(4)	Ni(2)−O(3)#4	2.036(4)
Ni(1)−F(1)#1	2.030(4)	Ni(2)−F(4)	2.026(3)
Ni(1)−F(2)#2	2.041(4)	Ni(2)−F(4)#4	2.029(4)
Ni(1)−F(2)	2.032(4)	Ni(2)−O(4)	2.097(4)
Ni(1)−O(1)	2.059(4)	S(1)−O(4)	1.482(4)
Ni(1)−O(2)	2.060(4)	S(1)−O(3)	1.489(4)
Ni(2)−F(3)#3	1.987(4)	S(1)−O(5)	1.459(4)
Ni(2)−F(3)	2.023(3)	S(1)−O(2)	1.480(4)

Bond Angles			
moiety	angle (deg)	moiety	angle (deg)
F(1)−Ni(1)−F(2)	87.52(14)	F(4)#4−Ni(2)−O(3)#4	84.8(2)
F(1)#1−Ni(1)−F(2)	79.1(2)	F(4)−Ni(2)−O(4)	85.37(14)
F(1)#1−Ni(1)−F(2)#2	170.36(12)	F(4)#4−Ni(2)−O(4)	97.70(14)
F(1)−Ni(1)−O(1)	90.6(2)	O(3)#4−Ni(2)−O(4)	98.2(2)
F(1)−Ni(1)−O(2)	168.7(2)	Ni(1)−F(1)−Ni(1)#2	101.1(2)
F(1)#1−Ni(1)−O(2)	97.0(2)	Ni(1)−F(2)−Ni(1)#1	100.7(2)
F(2)−Ni(1)−O(2)	94.5(2)	Ni(2)#4−F(3)−Ni(2)	95.9(2)
F(2)#2−Ni(1)−O(2)	89.9(2)	Ni(2)−F(4)−Ni(2)#3	94.5(2)
F(2)−Ni(1)−O(1)	69.9(2)	O(5)−S(1)−O(2)	109.5(3)
F(2)#2−Ni(1)−O(1)	95.7(2)	O(5)−S(1)−O(4)	109.4(3)
O(1)−Ni(1)−O(2)	89.3(2)	O(5)−S(1)−O(3)	109.6(3)
F(3)−Ni(2)−F(4)	85.12(14)	O(2)−S(1)−O(4)	108.7(2)
F(3)#3−Ni(2)−F(4)#4	73.94(14)	O(2)−S(1)−O(3)	108.4(3)
F(3)−Ni(2)−O(3)#4	91.3(2)	O(4)−S(1)−O(3)	111.2(2)
F(3)#3−Ni(2)−O(4)	88.2(2)	S(1)−O(2)−Ni(1)	134.5(3)
F(3)−Ni(2)−O(4)	70.5(2)	S(1)−O(3)−Ni(2)#3	131.8(3)
F (4)−Ni(2)−O(3)#4	75.9(2)	S(1)−O(4)−Ni(2)	131.5(2)

[a] Symmetry transformations used to generate equivalent atoms: #1, $-x+1, y-1, z-{}^1/_4$; #2, $x+1, -y+1, z+{}^1/_4$; #3, $-x+1, y, z-{}^1/_4$; #4, $x, -y+1, z+{}^1/_4$.

(1) = 2.01, Ni(2) = 1.93) and the average Ni−O/F bond lengths indicate the oxidation states of both the nickels to be +2 and S to be +6. The presence of the fluorine atoms finds indirect support from BVS calculations (F(1) = 0.614, F(2) = 0.607, F(3) = 0.66, F(4) = 0.62). Thus, the framework structure of $[Ni_2F_4(SO_4)\,H_2O]$ with a net framework charge of −2 is balanced by the protonation of the amine molecule.

The prominent feature of structure **II** is a dimer of edge-sharing octahedra. The Ni(1) and Ni(2) octahedral units share edges through fluorine (Ni(1)−F(1), F(2) and Ni(2)−F(3), F(4)) to form the dimer units $Ni_2(1)F_6O_2(H_2O)_2$ and $Ni_2(2)$-F_6O_4, respectively. The dimers are linked by sharing octahedral edges to form two distinct infinite sinusoidal chains along the [001] direction. These chains are alternately stacked one over the other along the [100] direction and are interlinked by sharing corners with the tetrahedral corners of the SO_4 groups to form a layer with an 11-membered aperture in the [101] plane (Figure 7b). To our knowledge, this is the first example of an 11-membered aperture in open-framework compounds. In the layer, each sulfate shares its three corners with three octahedra of the adjacent chains. It is connected to the Ni(1) octahedral chain by sharing one oxygen atom, whereas it shares two oxygen atoms with two neighboring octahedra of the Ni(2) chain. The layers thus formed are cross-linked by SO_4 tetrahedra along the *b*-axis through corner-sharing S−O−Ni linkages to form the three-dimensional structure (Figure 8). Such cross-linking of the layers forms an elliptical channel along the *c*-axis as shown in Figure 9. The width of the 10-membered channel is 12.3 × 6.12 Å (longest and shortest atom − atom compact distances, not including van der Waals radii). The channels are filled by the amine molecules which interact with the framework oxygen and fluorine through strong F−H···O and C−H···O hydrogen bonds. The structure of **II** is somewhat related to the mineral phosphoperite,[22] which contains layers of sinusoidal chains made up of edge-shared octahedral trimers cross-linked by tetrahedral PO_4 units.

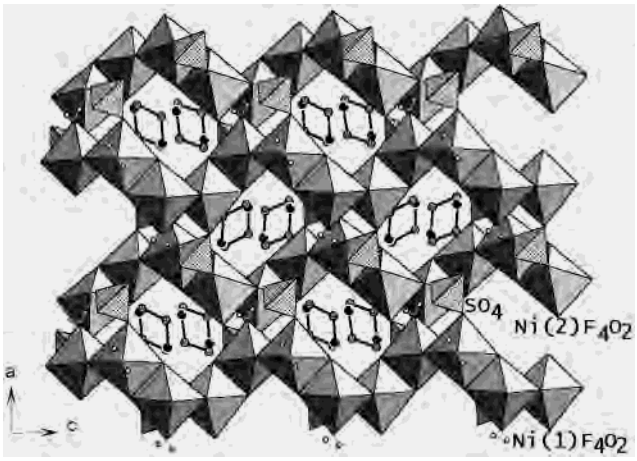

Figure 8. Polyhedral view of **II** along the [010] direction.

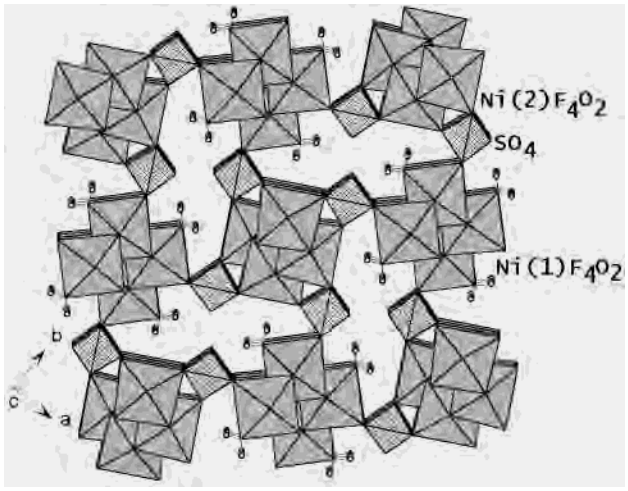

Figure 9. View down the crystallographic *c*-axis showing the inorganic framework structure of **II**, showing 10-membered channels.

The variable temperature magnetic susceptibility data at 5000 Oe of **II** are shown in Figure 10. The compound is predominantly paramagnetic and the inverse susceptibility data (see inset of Figure 10) show a linear behavior in the temperature range 50−300 K, yielding a small negative Curie temperature of −10 K, indicating weak antiferromagnetic interactions. The effective magnetic moment per nickel atom calculated from the linear fit of the χ_M^{-1} versus *T* curve is 2.3 μ_B, slightly lower than expected for Ni(II) centers (theoretical μ_{eff} = 2.83 μ_B). Zero-field-cooled (ZFC) and field-cooled (FC) susceptibility data (applied field of 500

(22) Huminicki, D. M. C.; Hawthorne, F. C. *Rev. Miner. Geochem.* **2002**, *48*, 193.

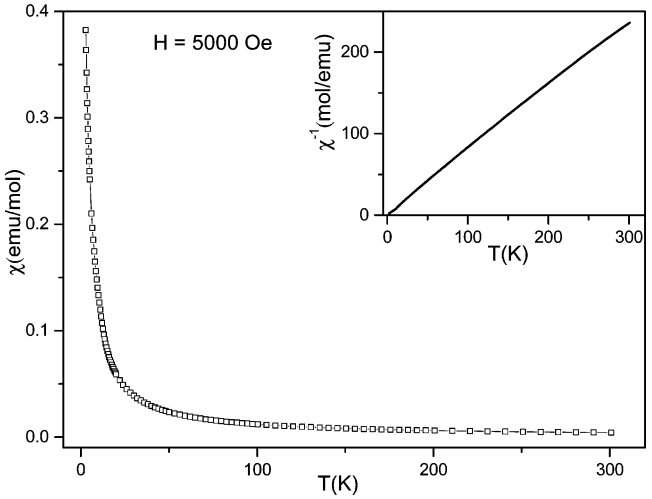

Figure 10. Temperature variation of the magnetic susceptibility of **II**. Inset shows the variation of inverse susceptibility.

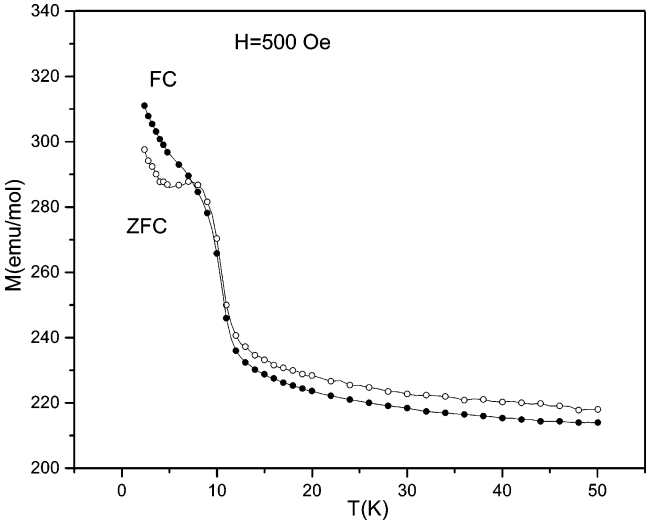

Figure 11. Temperature dependence of the DC magnetic susceptibility of **II** measured at 500 Oe under field-cooled (FC) and zero-field-cooled (ZFC) conditions.

Oe) shown in Figure 11 show only a slight divergence below 8 K. We did not observe magnetic hysteresis at 5 K.

Conclusions

Amine-templated Ni(II) sulfates of layered and 3D channel structures have been successfully synthesized under hydrothermal conditions, establishing thereby the versatility of the sulfate group in building open architectures. The magnetic behavior of the two nickel sulfates is interesting. The layered sulfate **I** with sinusoidal chains formed by hexameric units, containing three NiO(F) octahedra, shows ferrimagnetism. The 3D sulfate **II** with sinusoidal chains formed by dimeric units of NiO(F) octahedra is paramagnetic. Most Ni(II) compounds, specially the layered ones, are generally known to be antiferromagnetic. Dimensionality alone is not of much significance here as pointed out by Ferey and co-workers in the case of Ni(II) phosphates,[18] the most important factor being the way the NiO(F) octahedra are linked to one another. Ni(II) phosphates and other derivatives of Ni(II) with layered or 3D structures are antiferromagnetic.[19,23] Good examples of ferri- or ferromagnetic Ni(II) compounds are those of nickel succinate[24] and nickel glutarate[25] with unusual edge-sharing nickel octahedra. In the succinate, there are unusual hexanickel units: the polyhedron sharing two trans edges with two neighboring Ni_6 units. In the Ni_6 unit, a dimer of face-sharing octahedra is grafted onto a tetramer formed by two dimers of edge-sharing octahedra. The face-sharing nickel atoms are connected to the tetramer by edge-sharing with two adjacent nickel octahedra and corners with the opposite ones. In the glutarate, each nickel octahedron shares three edges with three nickel octahedra, each of which shares two of its edges with two neighboring nickel octahedra. The layered nickel sulfate $Ni_3(OH)_2(SO_4)_2(H_2O)$,[26] containing corrugated sheets formed by chains of NiO_6 octahedra, exhibits canted antiferromagnetism, with the three-dimensionality in this compound arising from the connectivity of the layers via the sulfate.

Supporting Information Available: TGA curves of **I** and **II**, hydrogen bonding interactions in **I** and **II**, and bond distances of structural analogues of **I** (pdf), and crystallographic data for **I** and **II** (cif). This material is available free of charge via the Internet at http://pubs.acs.org.

IC035488U

(23) (a) Guillou, N.; Gao, Q.; Nogues, M.; Morris, R. E.; Herview, M.; Ferey, G.; Cheetam, A. K. *C. R. Acad. Sci. Ser. IIc* **1999**, *2*, 387. (b) Guillou, N.; Gao, Q.; Forster, P. M.; Chang, J. S.; Nogues, M.; Park, S. E.; Ferey, G.; Cheetam, A. K. *Angew. Chem. Int. Ed.* **2001**, *40*, 2831. (c) Richard-Plouet, M.; Vilminot, S.; Guillot, M.; Kurmoo, M. *Chem. Mater.* **2002**, *14*, 3829. (d) Sanz, F.; Parada, C.; Rojo, J. M.; Ruiz-Valero, C. *Chem. Mater.* **2001**, *13*, 1334. (e) Goni, A.; Rius, J.; Insausti, M.; Lezama, L. M.; Pizarro, J. L.; Arriortua, M. I.; Rojo, T. *Chem. Mater.* **1996**, *8*, 1052.

(24) Guillou, N.; Livage, C.; Van Beek, W.; Nogues, M.; Ferey, G. *Angew. Chem. Int. Ed.* **2003**, *42*, 644.

(25) Guillou, N.; Livage, C.; Drillon, M.; Ferey, G. *Angew. Chem. Int. Ed.* **2003**, *42*, 5314.

(26) Vilminot, S.; Richard-Plouet, M.; Andre, G.; Swierczynski, D.; Bouree-Vigneron, F.; Kurmoo, M. *Inorg. Chem.* **2003**, *42*, 6859.